PNAS
www.pnas.org

Main Manuscript for

Evidence for biosurfactant-induced flow in corners and bacterial spreading in unsaturated porous media

Judy Q. Yang[a,c,d,*], Joseph E. Sanfilippo[b,e], Niki Abbasi[a], Zemer Gitai[b], Bonnie L. Bassler[b,f], and Howard A. Stone[a,*]

[a]Department of Mechanical and Aerospace Engineering, Princeton University, Princeton NJ 08544; [b]Department of Molecular Biology, Princeton University, Princeton NJ 08544; [c]Saint Anthony Falls Laboratory, University of Minnesota, Minneapolis MN 55414; [d]Department of Civil, Environmental, and Geo-Engineering, University of Minnesota, Minneapolis MN 55455; [e]Department of Biochemistry, University of Illinois at Urbana-Champaign, Urbana IL 61801; [f]Howard Hughes Medical Institute, Chevy Chase MD 20815

*Judy Q. Yang, Howard A. Stone.
Email: judyyang@umn.edu , hastone@princeton.edu

Author Contributions: J.Q.Y. and H.A.S. conceived the project and wrote the manuscript. J.Q.Y. and N.A. designed and performed the experiments. J.E.S. constructed the strains. All authors contributed to the experimental design, data analysis, and writing of the paper.
Competing Interest Statement: The authors declare no competing interests.
Classification: Biological Sciences/Microbiology, Physical Sciences/Environmental Sciences
Keywords: bacterial spreading | unsaturated porous media | corner flow | biosurfactant | wettability

This PDF file includes:
Main Text
Figures 1 to 4

Abstract

The spread of pathogenic bacteria in unsaturated porous media, where air and liquid coexist in pore spaces, is the major cause of soil contamination by pathogens, soft rot in plants, food spoilage, and many pulmonary diseases. However, visualization and fundamental understanding of bacterial transport in unsaturated porous media are currently lacking, limiting the ability to address the above contamination and disease related issues. Here, we demonstrate a previously unreported mechanism by which bacterial cells are transported in unsaturated porous media. We discover that surfactant-producing bacteria can generate flows along corners through surfactant production that changes the wettability of the solid surface. The corner flow velocity is on the order of several mm/h, which is the same order of magnitude as bacterial swarming, one of the fastest known modes of bacterial surface translocation. We successfully predict the critical corner angle for bacterial corner flow to occur based on the biosurfactant-induced change in the contact angle of the bacterial solution on the solid surface. Furthermore, we demonstrate that bacteria can indeed spread by producing biosurfactants in a model soil, which consists of packed angular grains. In addition, we demonstrate that bacterial corner flow is controlled by quorum sensing, the cell-cell communication process that regulates biosurfactant production. Understanding this previously unappreciated bacterial transport mechanism will enable more accurate predictions of bacterial spreading in soil and other unsaturated porous media.

Significance Statement

Here, we demonstrate a previously unreported mechanism of bacterial spreading in unsaturated porous media, which can inform understanding of soil contamination by pathogens, soft rot in plants, and potentially many pulmonary diseases. We discover that surfactant-producing bacteria establish self-generated flows along corners by producing surfactants that change the wettability of the solid surface. We validate this corner flow mechanism in a model soil consisting of packed grains. These results provide a mechanistic explanation for many previously non-understood observations that the spread of bacteria increases with increasing surfactants in soil and plants. In our experiments, the biosurfactant-driven corner flow has an average velocity of mm/h, which is significant in terms of the spread of bacteria, e.g., pathogens, in soil and other unsaturated porous media.

Main Text

Introduction

Bacteria are widely present in unsaturated porous media, where air and liquid coexist in pore spaces, such as in natural soils (1), plant tissues (2), food storage and packaging (3), and the lungs (4). The spread of pathogenic bacteria in these unsaturated porous media is the major cause of soil contamination by pathogens (5,6), soft rot in plants (7), food spoilage (8,9), and many pulmonary diseases (10). Fundamental understanding of the transport of bacterial cells in unsaturated porous media is key to addressing the above contamination and disease related issues. However, most current studies focus on bacterial transport in bulk liquids, driven by fluid advection, diffusion, and bacterial swimming and gliding motilities (11-14), and in liquid films on flat surfaces, due to solid-surface locomotion, biofilm expansion (15-19), and the production of a spatial gradients of biosurfactants that drive Marangoni flows, which are due to surface tension gradients (20-21). The transport of bacterial cells in unsaturated porous media, to our knowledge, has not been directly visualized and remains to be characterized.

Current understanding of bacterial transport in unsaturated porous media is primarily inferred from macroscopic observations and statistical analyses. For example, in soil science, researchers estimate the bacterial transport rate by injecting a bacterial solution into a sand column or aquifer for a short duration and then measure the concentration of bacterial cells at different distances, e.g., a few meters away from the injection site as a function of time (22-24). Many of these studies show that the transport of bacterial cells in soil increased after adding surfactants (24-26). In plant pathology, investigation of the invasion of bacterial mutants revealed that surfactant-producing bacteria cause more severe disease in host tissues or soft-rot (7). In addition, the development of many lung diseases is closely related to the functionality of some surfactant-producing genes (10, 27). The above observations highlight the importance of surfactants

in bacterial transport in unsaturated porous media. However, the mechanisms by which surfactants affect bacterial transport in these contexts are not clear.

Here, we demonstrate a previously unreported role of biosurfactants in inducing bacterial spreading in unsaturated porous media by generating corner flow. We discover that surfactant-producing bacteria generate flows along corners by producing surfactants that coat the solid surface and change its wettability. It has been known for decades that when a wetting liquid is placed in the corner region of a container or an angular pore, the air-water interface curves at the corner to maintain a constant contact angle at the solid surface, whose value is determined by the properties of the liquid and the solid surface (28-34). The triangular geometry of the corner requires the air-water interface to be concave when the sum of the contact angle and half the corner angle is less than $\pi/2$ (28,29). Classic corner flow theory suggests that when a wetting liquid forms a concave interface at the corner, a pressure gradient will build up along the corner due to the surface tension across the interface and the corner geometry (28-32). This pressure gradient generates a flow along the corner, which has been shown to play an important role in the transport of wetting liquids in soil (30,34). However, the transport of initially non-wetting liquids and bacteria, along corners and in soil, due to the production of biosurfactants that changes the contact angle has not been reported previously.

In this work, we first visualize bacterial flows in transparent, triangular prism-shaped chambers with different corner angles to mimic angular pores of unsaturated porous media. The material of the chamber, transparent polydimethylsiloxane (PDMS), is a compound with a silicon-oxygen main chain and hydrocarbon side chains, which acts as a surrogate for natural hydrophobic hydrocarbon-covered soils. We grow *Pseudomonas aeruginosa,* a typical biosurfactant-producing soil bacterium and major human pathogen, in water that initially does not wet the chamber, and we discover that this biosurfactant-producing bacterium can self-generate flows along corners, a phenomenon that, to our knowledge, has not been observed or suggested previously. Second, we demonstrate that the corner flow is induced by bacteria-produced biosurfactants and the corner geometry, rather than bacterial motility or the Marangoni effect. We successfully predict the critical corner angle for the bacterial corner flow to occur based on classic corner flow theory developed for pure uniform wetting liquids lacking bacteria. Third, we demonstrate biosurfactant-producing bacteria can indeed spread in a model soil, which consists of irregular PDMS grains packed in a confined space, while surfactant-deficient bacteria cannot. Finally, we demonstrate that the bacterial corner flow is controlled by quorum sensing, the cell-cell communication process that regulates biosurfactant production.

Results

Bacteria self-generate angle-dependent corner flow. To investigate whether and how bacteria are transported in a single angular pore space, we grew wild-type (WT) *P. aeruginosa* in modified M9 medium in a prism-shaped gas-permeable PDMS chamber with three different corner angles, namely 30°, 60°, and 90° (Fig. 1). The prism shape is a simplification of a macro-size pore in soil, which has corners, or corner-like shapes, formed between packed sand (0.05 – 2.0 mm) and gravel (> 2.0 mm). The modified M9 medium consists of M9 salts, 0.4% glucose, and micronutrients (see Methods). The WT cells harbored the green fluorescent protein (GFP) enabling visualization of the distribution of cells as the bacteria grew. The chamber was placed in a humidity- and temperature-controlled incubator, illuminated by a blue LED light, and imaged using a digital camera placed after a green light filter (see Methods). At t_g = 0 hours (h), the initial cell suspension had OD_{600} = 0.2-0.3. The bacteria grew for approximately 7 h, and a self-generated flow was observed at the 30° corner, but not at the 90° corner (Fig. 1 and Movie S1). A weak flow was observed at the 60° corner. No flow was observed in control experiments lacking cells (Movie S2), suggesting that it is the *P. aeruginosa* cells rather than the growth medium that generated the angle-dependent corner flow.

We note that after about 30-40 h of incubation, approximately 80% of the water had evaporated (Fig. S9). Thus, over the course of the corner flow (t_g = 7 – 12 h), we estimate that about 10% ($\approx \frac{5\text{h}}{40\text{h}} \times 80\%$) of the water evaporated. We expect that evaporation may affect our estimate of the speed of the bacterial corner flow by 10%.

We repeated the experiment eight times and observed similar corner flows at the 30° corner in all replicates. In contrast, corner flow observed at the 60° corner was not consistent, i.e., a weaker flow was observed at the 60° corner in some but not all replicate experiments (e.g., Movie S3). Furthermore, the flow at the 60° corner was suppressed if the initial cell density was increased to OD_{600} = 0.8 (Movie S4). Suppression of an induced flow likely occurs because at higher cell density, nutrients become depleted such that the level of surfactant, in this case rhamnolipids, produced diminishes (35-37). The experimental results suggest that there is a critical corner angle below which corner flow occurs and this critical angle is near 60°.

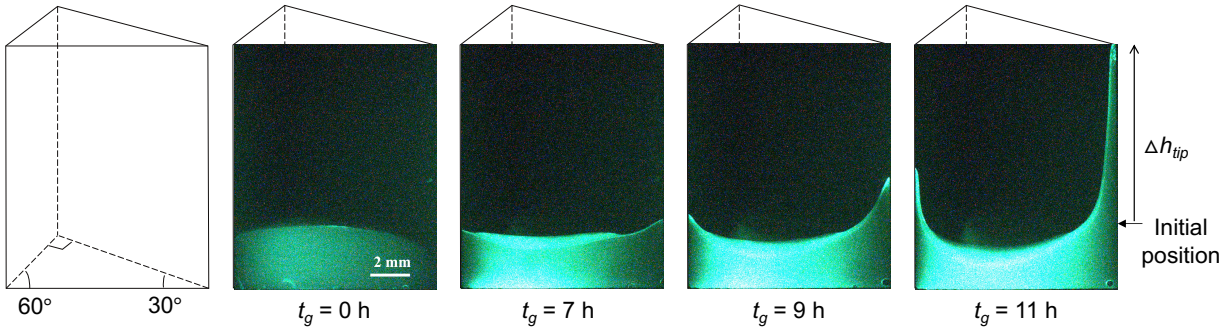

Fig. 1. *P. aeruginosa*, a soil bacterium and human pathogen, generated an angle-dependent corner flow. A liquid culture of cells labeled with GFP was placed in a prism-shaped gas-permeable PDMS chamber shown in the left-most sketch. t_g represents the time of bacterial growth in the chamber and Δh_{tip} represents the tip positions of the corner flows at the 30° corners relative to their initial positions at t_g = 0 h. The images became oversaturated after t_g = 7 h. The images were cropped so that the chamber height was 12.5 mm for consistency between different experiments shown in Fig. 2.

Bacterial corner flow is driven by biosurfactant production regulated by quorum sensing. To determine the mechanism underlying bacteria-driven corner flow, we carried out the above experiments with *P. aeruginosa* strains lacking flagella (Δ*fliC*), type IV pili (Δ*pilA*), the ability to retract type IV pili (Δ*pilTU*), biosurfactant production (Δ*rhlA*), and quorum sensing (Δ*lasR*). The flagella and pili enable motility of the bacteria; biosurfactants (rhamnolipids for *P. aeruginosa*) are compounds similar to other common surface-active materials that change the surface tensions of solutions and the contact angles on solid surfaces in contact with solutions (38); quorum sensing is a process of bacterial cell-cell communication that controls, among other processes, biosurfactant production in *P. aeruginosa* (39-40). The tip or front positions of the corner flows at the 30° corner (shown in Fig. 1) were plotted versus time for the wild-type cells and all of the mutants, as shown in Fig. 2(a).

Bacterial swimming and twitching motility, assisted by flagella and pili, respectively, have been recognized as common mechanisms for bacterial to self-spread in bulk liquids and saturated porous media (11-14). However, our experiments show that the WT strain and strains lacking motility (Δ*fliC*, Δ*pilA*, Δ*pilTU*) all generate corner flows at around t_g = 7 h, with little difference. This result indicates that the generation of corner flow where bacteria are observed to spread does not require bacterial motility.

In contrast to the negligible impact of bacterial motility on the bacterial corner flow, no corner flow occurred for the strain that was incapable of biosurfactant production (Δ*rhlA*) during the two-day incubation experiment (Fig. S2(b) and Movie S5). This result indicates that biosurfactants are required for bacterial self-generated corner flows. Recent studies show that bacteria can drive flows on flat surfaces by producing spatially heterogeneous distributions of biosurfactants that induce surface tension gradients, or a Marangoni flow (20-21). Therefore, it is possible that spatially heterogenous production and distribution of biosurfactants drove Marangoni flows at the corner. However, in the following sections we eliminate this Marangoni-related mechanism as a possible explanation for our results.

For the biosurfactant-producing bacteria, the WT strain, and strains lacking motility (Δ*fliC*, Δ*pilA*, Δ*pilTU*),

no corner flow occurred before t_g = 7 h, suggesting that bacteria must grow to sufficient cell density and/or produce sufficient amounts of biosurfactants to generate the corner flow. This hypothesis is consistent with the fact that biosurfactants are produced when the bacterial population reaches a particular threshold cell density, a process regulated by quorum sensing molecules called autoinducers (39,41). Moreover, a significant delay in the generation of corner flow occurred in the strain that was defective in quorum sensing (Δ*lasR*), which controls cell-density-dependent biosurfactant production (39,40). The movement of the Δ*lasR* strain at around t_g = 22 h is consistent with the fact that biosurfactant production is controlled by two quorum-sensing systems (Las and Rhl) such that deleting the *lasR* gene does not completely eliminate biosurfactant production because the Rhl system assumes control at later times (42-43). Thus, longer times are required to accumulate sufficient biosurfactant to generate the corner flow in the Δ*lasR* strain than the WT strain.

The speeds of the corner flows for the WT strain and the strains lacking motility were on average 1.6 mm/h, which is similar to the speed of bacterial swarming, one of the fastest modes of bacterial surface translocation known (19, 44). Compared with swarming that requires both biosurfactant production and bacterial motility (45, 46), the bacterial corner flow observed here only requires biosurfactant production. The observed flow speeds suggest that bacterial corner flows, as observed here, could induce significant fluid and bacterial fluxes in soil and other unsaturated porous materials where angular pores with corners are common (30, 47).

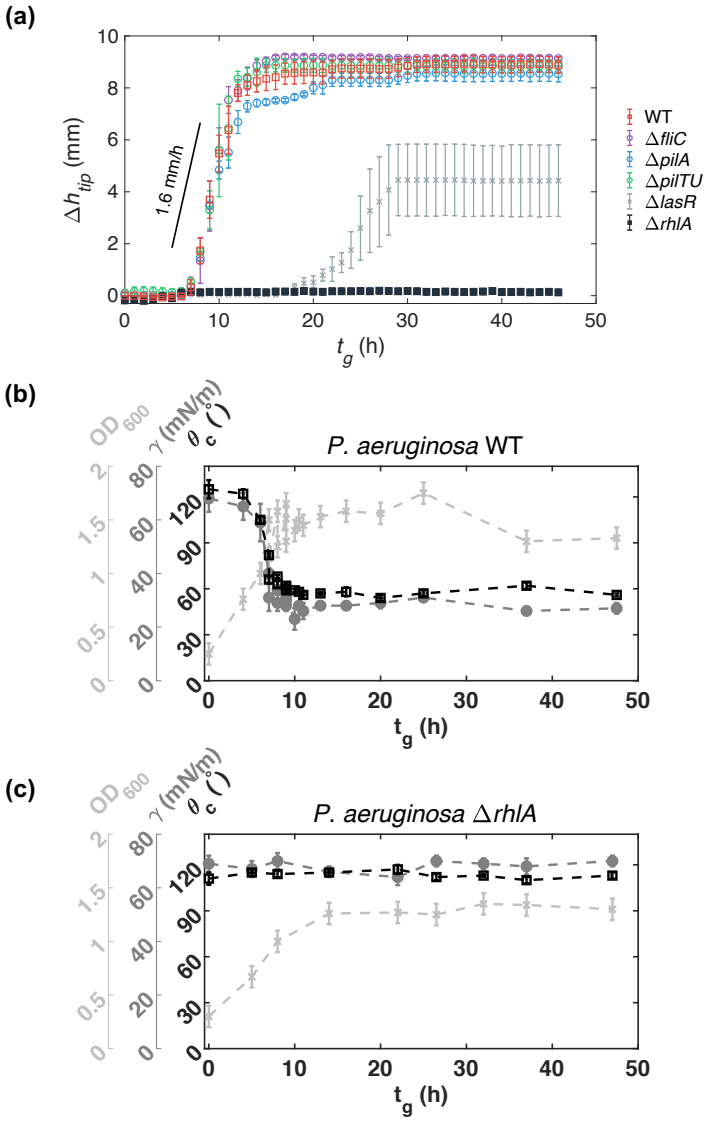

Fig. 2. Bacterial corner flow was induced by the production of biosurfactants, a process controlled by quorum sensing. (a) The time evolution of the tip positions of corner flows at the 30° corners, Δh_{tip} (Fig. 1), for different bacterial strains. The symbols and error bars represent the means and the standard errors, respectively, of at least two biological replicates for each bacterial strain. When the tip of the corner flows reached the upper boundary of the image, Δh_{tip} reached a plateau. Note that for consistency, the images for each experiment were cropped so that the chamber height is about 12.5 mm for each experiment. The black line shows the average velocity of the corner flows that occur during t_g = 7-12 h. (b) and (c) show the time evolution of the contact angle on the PDMS surface θ_c, the surface tension γ, and the cell density OD_{600}, of the solutions with WT and Δ*rhlA* cells, respectively. The error bar or uncertainty of OD_{600} was 0.1, the upper bound of the difference in OD_{600} between two biological replicates (see Methods). The uncertainties of γ and θ_c were calculated as the standard deviations of measurements of at least three liquid drops from the two culture samples combined together. The contact angle of the solution at t_g = 0 h was around 120°, similar to the angle reported for water on PDMS (48).

Corner flow occurs due to a biosurfactant-induced change in wettability of the solid surface. To understand how biosurfactants generate corner flow, we measured the time evolution of surfactant-related

parameters and the corresponding cell densities of the WT and Δ*rhlA* cultures. Specifically, we measured the contact angles (θ_c) on PDMS surfaces of the solutions, the surface tensions (γ) of the solutions, and the bacterial cell densities (OD_{600}) at different times as 5 mL cultures of bacteria grew in 50 mL culture tubes. The cells were grown under identical conditions as in the PDMS chamber, i.e., the same temperature, initial cell density, growth medium, and oxygen (see Methods). Note that we did not directly sample the solutions from the PDMS chamber because the volumes of the solutions in the chambers were too small to allow measurements of θ_c, γ, and OD_{600}. We caution that the cells might have grown somewhat differently in the culture tubes than in the PDMS chambers, but the general trends should be similar.

The time evolution of θ_c, γ, and OD_{600} for the WT and Δ*rhlA* strains are shown in Fig. 2(b) and (c), respectively. For the WT strain, θ_c and γ began to change dramatically around t_g = 6-7 h, which is the time window when corner flow began (Fig. 2(a)) and also the time when the bacterial culture achieved a cell density of $OD_{600} \approx 1$ (Fig. 2(b)). The coincidence in time supports the hypothesis that the bacterial corner flow was induced by biosurfactants produced exclusively at high cell density (38,39). Note that while our data show that *P. aeruginosa* cells produce biosurfactants in M9 medium (see Methods), we caution that *P. aeruginosa* only produces surfactants (rhamnolipids) when there is excess carbon (35-37). Furthermore, the corner flow was initiated when the contact angle of the solution on the PDMS surface changed from effectively non-wetting (θ_c > 90°) to wetting (θ_c< 90°), suggesting that the corner flow may be caused by a change in the wettability of the solid surface. The change in the wettability of the solid surface is likely caused by the sorption of the biosurfactant on both the air-water interface and the water-solid interface. In contrast to the WT strain, as the cells grew, no change in θ_c was observed for the Δ*rhlA* strain that is incapable of biosurfactant production (Fig. 2(c)), i.e., the PDMS surface was always non-wetting (θ_c > 90°). Consistent with the non-wetting of the solid surface, no corner flow was observed for the Δ*rhlA* strain (Fig. S2(b)), further suggesting that the biosurfactant-induced corner flow is likely caused by a change in the wettability or the contact angle of the solution on the solid surface.

The critical corner angle can be predicted by the contact angle using theories developed for homogeneous pure wetting liquids. To understand how bacteria generate corner flow by changing the wettability or the contact angle of the bacterial solution on a solid surface, we investigate the relationship between the critical corner angle (α_{crit}) below which corner flow occurs and the contact angle of the bacterial solution on the solid surface (θ_c). Specifically, we compared the relationship between α_{crit} and θ_c with classic corner flow theory developed for homogenous pure wetting liquids lacking cells or surfactants (29-33).

Classic corner flow theory suggests that pure homogeneous wetting liquids can flow along corners only if the corner angle, α, and contact angle of the pure wetting liquid on the solid surface, θ_c, satisfy $\alpha/2 + \theta_c < \pi/2$ (28). This result occurs because when $\alpha/2 + \theta_c < \pi/2$, based on the geometry, the air-water interface at the corner is concave (Fig. 3). According to force balance across a spherical interface, the relationship between the pressure in the solution p_{sol} and the pressure in the air p_{air} is $p_{sol} = p_{air} - \frac{2\gamma}{R}$, with R representing the radius of curvature (in a plane, this is the radius of an inscribed circle). This equation means that the smaller R the smaller the p_{sol}; thus, as the height z increases along the corner, p_{sol} decreases because R decreases. This decrease of the pressure in the solution with increasing z, i.e., $\frac{\partial p_{sol}}{\partial z} < 0$, drives flow along the corner (29-33). In contrast, if $\alpha/2 + \theta_c > \pi/2$, the air-liquid interface will be convex, such that $p_{sol} = p_{air} + \frac{2\gamma}{R}$ and p_{sol} increases with increasing z, and thus no corner flow will occur because liquids flow from high pressure to low pressure.

According to the classic corner flow criterion ($\alpha/2 + \theta_c < \pi/2$), if we assume the bacterial solution is homogeneous, then to generate corner flow, the corner angle α must be smaller than a critical angle $\alpha_{crit} = 2(\pi/2 - \theta_c)$. In our experiments with surfactant-producing WT *P. aeruginosa*, the corner flow occurred when the contact angle changed from $\theta_c \approx 120°$ to $\theta_c \approx 60°$ at $t_g \approx 7$ h (Fig. 2(b)). At t_g < 7 h, $\theta_c \approx 120°$, such that $\alpha_{crit} = 2(\pi/2 - \theta_c) < 0°$, which is physically impossible, thus no corner flow would occur. Once the biosurfactant changed the contact angle to $\theta_c \approx 60°$ (t_g > 7 h), the critical corner angle becomes $\alpha_{crit} = 2(\pi/2 - \theta_c) \approx 60°$, suggesting that corner flow only occurs at $\alpha < \alpha_{crit} \approx 60°$. Consistent with this supposition, at t_g < 7 h, we observed no corner flow, and at t_g > 7 h, we observed no flow at 90°, a weak

flow at 60°, and significant and consistent corner flow at the 30° corner (Fig. 1). Our direct observations of corner flow also suggest that the critical corner angle to generate corner flow is 60°. The agreement between our observed α_{crit} and the α_{crit} predicted using the corner flow criterion based on the measured θ_c confirms our hypothesis that bacterial corner flow is caused by the biosurfactant-induced change in contact angle θ_c, or the wettability of the solid surface. Furthermore, the corner flow criterion assumes a uniform surface tension: thus, the agreement between our observed α_{crit} and the predicted α_{crit} also suggests that bacterial corner flow is driven by the corner geometry, which induces a gradient in the air-water interface curvature along the corner, and is not driven by the Marangoni effect, or a spatial gradient of surfactants or surface tension.

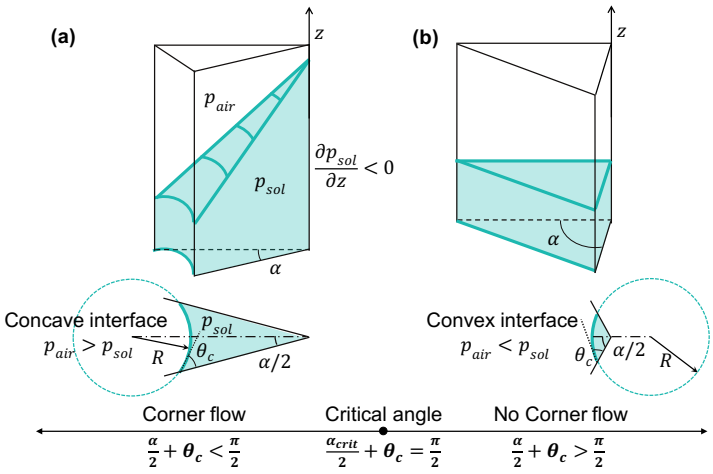

Fig 3. Criterion for generation of corner flow for homogeneous wetting liquids. (a) Given the contact angle of a solution on a solid surface θ_c, corner flows occur when the corner angle α satisfies $\alpha/2 + \theta_c < \pi/2$, such that the air-water interface is concave. A concave interface demands that the pressure in the solution is lower than the pressure in the air, $p_{air} > p_{sol}$, such that a negative pressure gradient forms in the vertical (z) direction, $\frac{\partial p_{sol}}{\partial z} < 0$. This pressure gradient drives corner flow. (b) No corner flows occur when $\alpha/2 + \theta_c > \pi/2$, because, under this condition, the air-water interface is convex such that $p_{air} < p_{sol}$ so no negative pressure gradient exists in the z direction.

Corner flow likely occurs in unsaturated porous media. To test our hypothesis that the Marangoni effect, or a surface tension gradient, is not required for the bacterial corner flow observed in our experiments, we conducted corner flow experiments using homogeneous solutions with biosurfactant present but no cells. Specifically, we obtained the bacterial solution from WT *P. aeruginosa* at t_g = 13 h, when the contact angle on PDMS and the surface tension of the solution had reached equilibrium (Fig. 2(b)). After removing the bacterial cells using a 0.2 μm filter and adding a small amount of a fluorescently labeled molecule (0.004 % 2-NBDG glucose) to the solution (see Methods), we homogenized the cell-free culture fluid using a vortex mixer so that any biosurfactant would be uniformly distributed, i.e., there should be no surface tension gradient. We transferred this homogeneous solution into the prism-shaped chamber and imaged the resulting fluorescence of the fluid in the chamber (Fig. 4(a)). Immediately after the fluid was transferred into the chamber t_{in} = 0, corner flow began to occur at the 30° corner, but no flow occurred at the 90° corner and only a weak flow occurred at the 60° corner. The corner flow that occurred in the homogenous solution lacking any cells was similar to that that occurred when growing cells were present (Fig. 1), indicating that bacterial corner flow is driven by the curvature gradient at the corner and not by a surface tension gradient. Therefore, the mechanism that transports bacteria at corners that we have identified is distinct from that previously reported for bacterial flows driven by the Marangoni effect, or by surface tension gradients (20-21).

The fact that biosurfactant solutions lacking cells generated corner flows is consistent with our observation that mutants lacking motility also generated corner flows (Fig. 2(a)), while cells incapable of biosurfactant production did not (Figs. 2(c) and S1(b)). Thus, corner flows are driven by biosurfactants that bacteria

produce or, possibly in natural settings, that are produced by other bacterial cells in the vicinal community. Biosurfactants are "public goods", compounds that, because they are released, can be accessed by all members of a community irrespective of whether or not a particular member participated in their production (36,37,49). To explore whether biosurfactants are public goods that can be exploited to enhance bacterial spreading, we carried out our corner flow experiment using a mixture of 50% WT *P. aeruginosa* cells without GFP and 50% Δ*rhlA* cells with GFP. As shown in Fig. 4(c), the Δ*rhlA* cells with GFP were transported with the corner flow generated by the WT cells, which started at around t_g = 9 h. The delay of the start time of the corner flow compared to the case with 100% WT cells (Fig. 1) is presumably a consequence of only half of the cells producing biosurfactant. The transport of Δ*rhlA* cells with the WT cells suggests that biosurfactants are indeed public goods that benefit all bacteria in terms of spreading, possibly in soil and other niches with corners or other similar narrow geometries. Therefore, quorum-sensing-controlled biosurfactants may provide a survival benefit to bacteria by facilitating their dissemination to new territory when the cell density becomes high (36,37,49).

We anticipate that the previously unreported mechanism of bacterial transport, due to the production of biosurfactants, the change of surface wettability, and corner geometry, is widely present in unsaturated porous media, such as soils, where angular pores with corners are common (30, 47). To test our hypothesis, we simulated a soil by packing angular PDMS grains, with grain size d_s ranging from 0.5 to 1.0 mm, in a confined cuboid-shaped PDMS chamber. The four corner angles of the chamber are 90° such that no corner flow is generated along the corners of the chamber. The model soil was placed above a drop of bacterial solution with initial OD_{600} = 0.2-0.3. Bacterial solutions consisting of WT *P. aeruginosa* with GFP and Δ*rhlA* cells with GFP were incubated separately in duplicate soil chambers and the experiments were repeated four times. Similar to the corner flow experiments shown in Fig. 1, the soil chambers were placed in a humidity- and temperature-controlled incubator and imaged from the front of the chamber. After incubation for 12 h, only the surfactant-producing WT cells penetrated into the soil, while the surfactant-deficient Δ*rhlA* cells did not (observed all four times), showing that bacterial cells can indeed be transported in unsaturated porous media, such as soil, by producing biosurfactants. This biosurfactant-driven bacterial transport in a model soil demonstrates that the previously unreported bacterial transport mechanism we imaged in a model angular pore, due to the generation of surfactants that drive corner flow after altering the wettability of the solid surface, is present in unsaturated porous media such as soil.

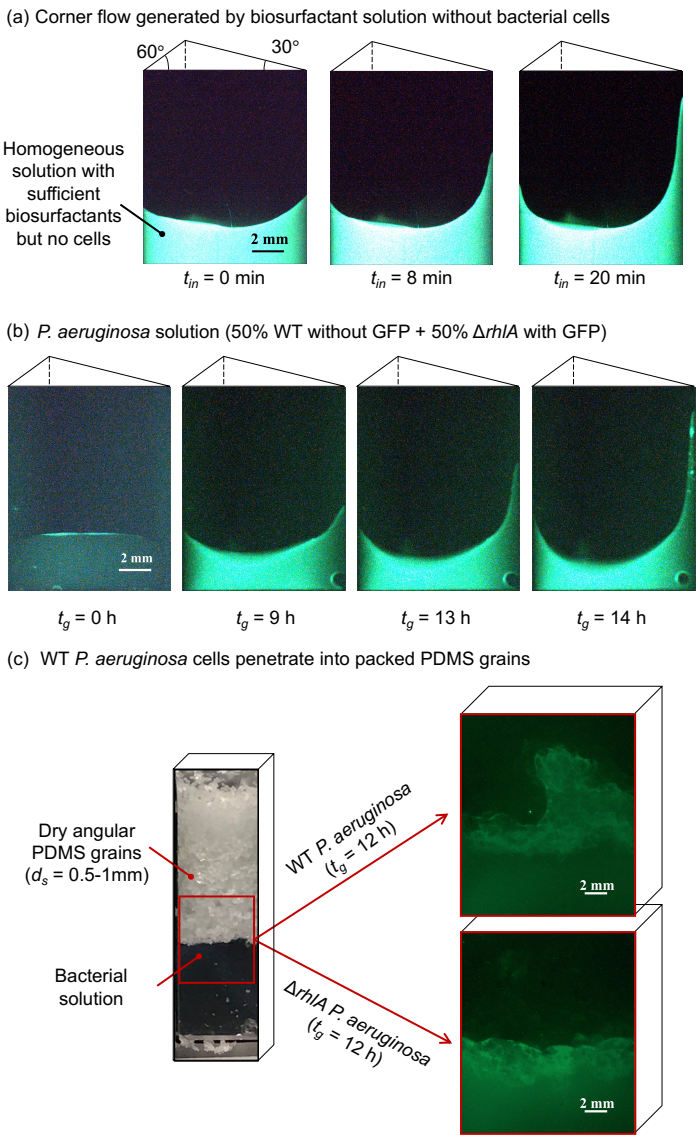

Fig. 4. Corner flow is a previously unappreciated mechanism of bacterial transport and occurs in unsaturated porous media. (a) A homogenous biosurfactant solution lacking cells drives corner flow. The solution was composed of cell-free culture fluid prepared from WT *P. aeruginosa* grown for 13 h, such that the contact angle for the homogenous solution had reached equilibrium (Fig. 2(b)). t_{in} = 0 min indicates the time when the solution was transferred into the PDMS chamber. Fluorescence visualization was achieved by the addition of 0.004% fluorescent 2-NBDG glucose. (b) Surfactant-deficient bacteria (Δ*rhlA*) are transported with the corner flow generated by surfactant-producing WT bacteria. The experimental setup is similar to that in Fig. 1, except that the solution is a mixture of 50% WT *P. aeruginosa* without GFP and 50% Δ*rhlA* cells harboring GFP. The black circle at the lower right corner of the chamber is a bubble, possibly generated from evaporation. (c) Bacterial surfactants drive bacterial spreading in a model soil, which consists of dry angular PDMS grains packed in a confined chamber placed above a drop of bacterial solution. t_g represents the time of bacterial growth in the chamber and the initial bacterial culture had OD_{600} = 0.2-0.3.

Discussion

We have documented a here-to-fore unrecognized bacterial transport mechanism, i.e., bacteria can self-generate flows along corner-like geometries by producing biosurfactants that change the contact angle of

liquid on solid surfaces. In addition, we quantitatively predicted the critical corner angle for the bacterial corner flow to occur based on the changes in contact angle due to bacterial biosurfactant production. Furthermore, we demonstrated similar bacterial surfactant-driven transport in a typical unsaturated porous media, in this case, a model soil of packed angular grains. This previously unreported mechanism provides a mechanistic basis for rationalizing many previous unsolved puzzles: the observations that surfactants enhance bacterial transport in soil (24-26), and that the soft rot of plants is closely linked to bacteria that harbor genes encoding surfactant biosynthetic components (7).

We anticipate that the bacterial transport mechanism documented here plays an important role in the spreading of bacteria in unsaturated porous media, because the speed of the observed bacterial corner flow is on average 1.6 mm/h, which is the same magnitude as bacterial swarming, one of the fastest modes of bacterial surface translocation known (19, 44). Further, the spread of pathogens in soil and the development of plant and human lung diseases often occur over days to months (7, 50, 51), thus the corner flow with velocity about 1.6 mm/h or 4 cm/day (or 1 m/month) is significant considering that the length scales of many plants, human organs, and soil areas are on the order of tens of centimeters to meters. This biosurfactant-induced bacterial spreading mechanism has not been incorporated into current bacterial transport models, which consider advection, diffusion, bacterial motility, and Marangoni effects (21, 52, 53). Therefore, the spreading of microbes in unsaturated porous materials may have been significantly underestimated in current studies. The transport mechanism identified here could underpin improved predictions and simulations of bacterial spreading in soils and the associated biogeochemical cycle, which is a function of bacterial biomass (54-56), as well as improve predictions of the spreading of pathogenic bacteria in soil, plants, and other unsaturated porous media such as human tissues.

Our results suggest that biosurfactants and quorum-sensing molecules provide survival benefits to bacteria by facilitating their dissemination to new territory when cell density becomes high. This phenomenon may explain the existence of a large variety of biosurfactant-producing bacteria in many unsaturated porous media, such as soil (57). Furthermore, the corresponding transport of surfactant-deficient bacteria, as free-riders when present with surfactant-producing bacteria, shows that biosurfactants are public goods, consistent with previous studies (36,37,49), and moreover, that transport does not necessitate that a particular bacterium be capable of either motility or biosurfactant production.

Finally, biosurfactants produced by *P. aeruginosa*, rhamnolipids, are biodegradable (58). Thus, our results also suggest that it may be possible to enhance bioremediation outcomes by using rhamnolipid-producing bacteria or adding rhamnolipids to bioremediation solutions to enhance the transport of bacterial-biodegraders that do not themselves make biosurfactants. Furthermore, in addition to rhamnolipids, other biosurfactants, such as glycolipids produced by *Lactococcus lactis*, can also make some initially non-wetting surfaces into wetting surfaces (59, 60). Therefore, we anticipate that biosurfactants produced by other bacteria may similarly enable relatively rapid bacterial transport in unsaturated porous materials.

Materials and Methods

Strains and growth conditions. The bacterial strains and primers used in this study are described in Table S1. *P. aeruginosa* was grown in liquid LB in a roller drum, and on LB agar (1.5% Bacto Agar) at 37°C. Gentamicin (Sigma) was used at 30 µg/mL. The *rhlA* deletion construct was generated by the lambda Red recombinase system using the *aacC1* ORF between the flanking regions of the targeted gene of interest (61).

Bacterial solution. We grew *P. aeruginosa* strains from frozen stocks in LB overnight (around 16 h). Cultures were subjected to centrifugation at 4,000 rpm for 10 min in a 10 mL tube. After withdrawing the supernatant from the tube, the bacterial pellet was resuspended in M9 medium at an OD_{600} = 0.2 - 0.3. The M9 medium used here included 0.4% D-glucose and was supplemented with 0.03 µM $(NH_4)_6(Mo_7)_{24}$, 4 µM H_3BO_3, 0.3 µM $CoCl_2$, 0.1 µM $CuSO_4$, 0.8 µM $MnCl_2$, 0.1 µM $ZnSO_4$, and 0.1 µM $FeSO_4$. When noted, 0.004% (w/v) fluorescent 2-NBDG glucose was added.

Fabrication of the PDMS chambers and grains. The PDMS liquid was prepared by mixing PDMS base elastomer and curing agent (Dow Sylgard 184) at a 1 to 0.075 ratio. We molded the PDMS chambers by

pouring uncured PDMS liquid into a petri dish with molds of different shapes. For the triangular prism-shaped chamber, the mold was a laser-cut prism-shaped aluminum mold (4 mm height of the cross-sectional triangle and 2 cm chamber height). For the cuboid chamber, the mold (1 cm length by 4 mm width by 3 cm height) was printed using a 3D printer (Formlabs Inc., MA, USA) using standard grey resin. The petri dish was placed in a 60 °C oven for about 2.5 h. After curing and cooling, extra PDMS around the prism mold was eliminated and the PDMS chamber was removed from the mold.

To prepare PDMS grains, the same PDMS liquid was poured into a petri dish and cured. Subsequently, the slabs were cut into smaller pieces and placed inside a coffee grinder (Cuisinart DBM-8 Supreme Grind, Cuisinart, CT, USA) to prepare PDMS grains. The PDMS grains were ground at the finest grain size setting, and microscopic images show that ground grains resembled angular sand with a size distribution of about 0.5 – 1 mm (Fig. S8). Subsequently, the PDMS grains were collected and placed in 70% ethanol overnight for sterilization.

Corner flow experiment. At the start of experiments, such as that shown in Fig. 1, we transferred 55 µL of the prepared bacterial culture at OD_{600} = 0.2-0.3 into a PDMS chamber using a pipette. The inoculated chamber was placed in an incubator with a transparent front door, temperature 36 ± 2 °C, and relative humidity 80 ± 10%. To visualize the bacterial-induced corner flow, we illuminated the PDMS chamber from the front using a collimated beam of blue light (wavelength 475 ± 18 nm). The beam size was significantly larger than the chamber size to ensure that the entire bacterial culture was uniformly illuminated. Upon excitation by blue light, *P. aeruginosa* harboring GFP or the solution containing fluorescent 2-NBDG glucose emitted green light that could be quantified by passage through a 530 ± 22 nm filter (M470L4, Thorlabs, Inc., NJ, USA). Emission was recorded over time using a digital camera (Blackfly S BFS USB3, Teledyne FLIR, OR, USA) with a macro lens (105 mm 1:2.8 DG Macro, Sigma, NY, USA) at 1 to 2 min intervals between image acquisitions for 2 days. The distance from the lens to the filter set was 2.5 cm, and the distance from the filter to the sample was about 15 cm. An image of the experimental setup and schematic diagrams are shown in Fig. S1. Note that while the height of the prism-shaped chamber is about 2 cm, only a portion of the chamber height is captured by the camera due to limited field of view. To keep the results consistent, we cropped the images and maintained the chamber height around 12.5 mm for each experiment shown in Fig. 2(a). Only a subset of data was shown in Fig. 2(a) for visual clarity. The tip positions of the corner flows were estimated by image processing using routines in MATLAB by first identifying the bacterial culture via analysis of the fluorescence intensity of the image with a threshold cutoff, and subsequently, identifying the top position of the culture near the corner. The link to the MATLAB codes is shared at the end of the Methods section.

For the corner flow with the Δ*lasR* strain (Fig. 2(a)), the amplitude of the corner flow, which started one day after initiation of the experiment, may be affected by evaporation that occurred over the 2 days (Fig. S9). However, we anticipate that the starting time of the corner flow should not be affected by evaporation because experiments with different humidities (>50%) and different amounts of liquid in the chamber had similar starting times. The identical setup was used to record the corner flow of a solution lacking bacterial cells (Fig. 4(a)). In order to capture the rapid motion of the corner flow in the experiment in Fig. 4(a), the solution was transferred into the chamber using a needle and a tube connected to a 1 mL syringe instead of a pipette. Because the resolution of the syringe is 5 µL and there was likely an empty space in the needle before the injection of the solution, the volume of the solution transferred in the chamber may not be exactly 55 µL. The volume of the solution should not affect the results because the solution was homogenized.

Bacterial transport in a model soil experiment. The bacterial solutions were prepared as described as above. 400 µL of each solution was transferred to the cuboid shaped chamber using a pipette. Next, 0.6 g of PDMS grains were transferred and packed manually, using a lab spatula, over the top of solutions inside each chamber. The grains were packed such that the bottom layer of the PDMS grains came in contact with the liquid solution in the chamber. The chamber was placed in the same incubator and imaged using the same imaging system as in the corner flow experiments.

Contact angle and surface tension measurements. We measured the contact angle θ_c, surface tension γ, and bacterial cell density (OD_{600}). Because the amount of solution in the PDMS chamber (< 100 µL) made direct sampling impossible, we used bacterial cultures grown in 50 mL centrifuge tubes when aliquots

were needed. Specifically, we grew 5 mL of *P. aeruginosa* cultures (OD_{600} = 0.2-0.3) in 50 mL tubes and placed the tubes in a 200 rpm shaking incubator at 36 ± 2 °C to mimic the corner flow experiments. To study the time evolution of OD_{600}, γ , and θ_c, at each sampling time, two bacterial culture tubes were removed from the incubator. We first transferred 600 µL of bacterial culture from each tube to cuvettes and measured the OD_{600}. Each OD_{600} data point in Fig. 2(b) and (c) represents the average of the cell densities in the two sample tubes. The error bar/uncertainty of each OD_{600} data point was 0.1, the upper bound of the difference in the cell densities of the two samples. As a reference, we estimated, using colony forming units, that the number of viable cells for a bacterial culture of maximum $OD_{600} \approx 1.6$ is around 10^{10} cells/mL. Given that the shape of *P. aeruginosa* is a rod of 1-5 µm length and 0.5-1 µm diameter, we estimated that the volume fraction of the bacteria in the solution at $OD_{600} \approx 1.6$ was around 0.2 - 4%.

To measure γ and θ_c, we first combined the two bacterial cultures sampled at each time point. To remove bacterial cells, we subjected the samples to centrifugation at 10,000 rpm for 10 min. The supernatant was filtered through a 0.2 µm filter. We transferred the filtered solution into a syringe with an 18-gauge needle. To measure the surface tension γ of the filtered solution, we gently forced a drop out of the syringe, and recorded the shape of the pendant drop below the needle. γ was estimated by fitting the profile of the drop edge to an analytical profile based on the algorithm proposed by Rotenberg et al. (62) using the MATLAB code developed by the Stone group. The advancing contact angle θ_c was estimated using the same solution. In this case, we placed the syringe on a syringe pump connected to a needle on top of a PDMS surface. The PDMS surface was produced identically to the PDMS chambers. We forced the solution out of the syringe using the pump at 1-20 µL/min and recorded the shape of the moving drops on the PDMS surface using a digital camera. After identifying the edges of the moving drops, we estimated θ_c as the angle between the PDMS surface and the tangent line of the drop edge near the contact line. The MATLAB codes for image processing and the estimation of surface tension and contact angle are shared on github: https://github.com/JudyQYang/Bacterial_corner_flow_codes.

Acknowledgments

This research was supported by the Princeton Environmental Institute, through the Grand Challenges program and the Carbon Mitigation Initiative, and the NSF grant MCB-1853602 (B.L.B. and H.A.S.). B.L.B. is supported by the Howard Hughes Medical Institute. The authors thank Dr. J. Yan for insightful discussions and Dr. J. Valastyan for help with the bacterial strains.

References

1. CP Gerba, C Wallis, JL Melnick, Fate of wastewater bacteria and viruses in soil in *J. Irrigat. Drainage Div. ASCE*. pp. 157–174 (1975).
2. J. Mansfield *et al.*, Top 10 plant pathogenic bacteria in molecular plant pathology. *Mol. Plant Pathol* **13**(6), 614-629 (2012).
3. L Gram, L Ravn, M Rasch, JB Bruhn, AB Christensen, and M Givskov, Food spoilage—interactions between food spoilage bacteria. *Int. J. Food Microbiol.* **78**(1-2), 79-97 (2002).
4. RP Dickson, FJ Martinez, and GB Huffnagle, The role of the microbiome in exacerbations of chronic lung diseases. *The Lancet* **384**(9944), 691-702 (2014).
5. A Schäfer, *et al.*, Transport of bacteria in unsaturated porous media. *J. Contam. Hydrol.* **33**(1-2), 149-69 (1998).
6. M Conboy, M Goss, Natural protection of groundwater against bacteria of fecal origin. *J. Contam. Hydrol.* **43**, 1–24 (2000).
7. AM Hernandez-Anguiano, TV Suslow, L Leloup, CI Kado, Biosurfactants produced by *Pseudomonas fluorescens* and soft-rotting of harvested florets of broccoli and cauliflower. *Plant Pathol.* **53**(5), 596-601 (2004).
8. L Gram, *et al.*, Food spoilage - interactions between food spoilage bacteria. *Int. J. Food Microbiol.* **78**, 79–97 (2002).
9. P Dalgaard, Qualitative and quantitative characterization of spoilage bacteria from packed fish. *Int. J. Food Microbiol.* **26**, 319–333 (1995).
10. AM Pastva, JR Wright, KL Williams. Immunomodulatory roles of surfactant proteins A and D: implications in lung disease. *P. Ann. Am. Thorac.* **4**(3), 252-7 (2007).
11. RM Macnab, SI Aizawa, Bacterial motility and the bacterial flagellar motor. *Annu. Rev. Biophys. Bioeng.* **13**, 51–83 (1984).

12. K Son, DR Brumley, R Stocker, Live from under the lens: exploring microbial motility with dynamic imaging and microfluidics. *Nat. Rev. Microbiol.* **13**, 761–775 (2015).
13. A Siryaporn, MK Kim, Y Shen, HA Stone, Z Gitai, Colonization, competition, and dispersal of pathogens in fluid flow networks. *Curr. Biol.* **25**, 1201–1207 (2015).
14. T Bhattacharjee, SS Datta, Bacterial hopping and trapping in porous media. *Nat. communications* **10**, 1–9 (2019).
15. RM Harshey, Bacterial motility on a surface: many ways to a common goal. *Annu. Rev. Microbiol.* **57**, 249–273 (2003).
16. J Yan, CD Nadell, HA Stone, NS Wingreen, BL Bassler, Extracellular-matrix-mediated osmotic pressure drives vibrio cholerae biofilm expansion and cheater exclusion. *Nat. Commun.* **8**, 1–11(2017).
17. N Verstraeten, *et al.*, Living on a surface: swarming and biofilm formation. *Trends Microbiol.* **16**, 496–506 (2008).
18. Y Wu, HC Berg, Water reservoir maintained by cell growth fuels the spreading of a bacterial swarm. *Proc. Natl. Acad. Sci.* **109**, 4128–4133 (2012).
19. J Yan, H Monaco, JB Xavier, The ultimate guide to bacterial swarming: an experimental model to study the evolution of cooperative behavior. *Annu. Rev. Microbiol. 73*, 293–312 (2019).
20. TE Angelini, M Roper, R Kolter, DA Weitz, MP Brenner, Bacillus subtilis spreads by surfing on waves of surfactant. *Proc. Natl. Acad. Sci.* **106**, 18109–18113 (2009).
21. M Fauvart, et al., Surface tension gradient control of bacterial swarming in colonies of *Pseudomonas aeruginosa*. *Soft Matter* **8**, 70–76 (2012).
22. RW Harvey, LH George, RL Smith, DR LeBlanc. Transport of microspheres and indigenous bacteria through a sandy aquifer: results of natural-and forced-gradient tracer experiments. *Environ. Sci. Technol.* **23**(1), 51-6 (1989).
23. G Bai, ML Brusseau, RM Miller, Influence of a rhamnolipid biosurfactant on the transport of bacteria through a sandy soil. *Appl. Environ. Microbiol.* **63**, 1866–1873 (1997).
24. H Zhong, *et al*., Transport of bacteria in porous media and its enhancement by surfactants for bioaugmentation: a review. *Biotechnol. Adv.* **35**, 490–504 (2017).
25. DK Powelson, AL Mills, Water saturation and surfactant effects on bacterial transport in sand columns. *Soil Sci*. **163**(9), 694-704 (1998).
26. G Chen, M Qiao, H Zhang, H Zhu, Bacterial desorption in water-saturated porous media in the presence of rhamnolipid biosurfactant. *Res. Microbiol*. **155**(8), 655-61 (2004).
27. RJ. King, Pulmonary surfactant. *J. Appl. Physiol.* **53**(1), 1-8 (1982).
28. P Concus, R Finn, On the behavior of a capillary surface in a wedge. Proc. Natl. *Acad. Sci. United States Am.* **63**, 292 (1969).
29. MM Weislogel, Capillary flow in an interior corner. *J. Fluid Mech.* **373**, 349–378 (1998).
30. M Tuller, D Or, Hydraulic conductivity of variably saturated porous media: Film and corner flow in angular pore space. *Water Resour. Res.* **37**(5), 1257-76 (2001).
31. Higuera FJ, Medina A, Linan A. Capillary rise of a liquid between two vertical plates making a small angle. *Phys. Fluids* **20**(10), 102102 (2008).
32. A Ponomarenko, D Quéré, C Clanet, A universal law for capillary rise in corners. *J. Fluid Mech.* **666**, 146–154 (2011).
33. MM Weislogel, Compound capillary rise. *J. Fluid Mech.* **709**, 622–647 (2012).
34. Hoogland F, Lehmann P, Mokso R, Or D. Drainage mechanisms in porous media: From piston-like invasion to formation of corner flow networks. *Water Resour. Res.* **52**(11), 8413-36 (2016).
35. KE Boyle, H Monaco, D van Ditmarsch, M Deforet, JB Xavier. Integration of metabolic and quorum sensing signals governing the decision to cooperate in a bacterial social trait. *PLoS Comput Biol.* **11**(6):e1004279 (2015).
36. JB Xavier, W Kim, KR Foster. A molecular mechanism that stabilizes cooperative secretions in *Pseudomonas aeruginosa*. *Mol. Microbiol*. **79**(1), 166-79 (2011).
37. B Mellbye, M Schuster, Physiological framework for the regulation of quorum sensing-dependent public goods in *Pseudomonas aeruginosa*. *J. Bacteriol*. **196**(6), 1155 (2014).
38. G Soberón-Chávez, F Lépine, E Déziel, Production of rhamnolipids by pseudomonas aeruginosa. *Appl. Microbiol. Biotechnol.* **68**, 718–725 (2005).
39. S Schauder, BL Bassler, The languages of bacteria. *Genes Dev* **15**, 1468–1480 (2001).
40. ST Rutherford, BL Bassler, Bacterial quorum sensing: its role in virulence and possibilities for its

control. *Cold Spring Harb. Perspectives Medicine* **2**, a012427 (2012).
41. DH Dusane, *et al*., Quorum sensing: implications on rhamnolipid biosurfactant production. *Biotechnol. Genet. Eng. Rev.* **27**, 159–184 (2010).
42. V Dekimpe, E Deziel, Revisiting the quorum-sensing hierarchy in *Pseudomonas aeruginosa*: the transcriptional regulator *rhlr* regulates *lasr*-specific factors. *Microbiol.* **155**, 712–723 (2009).
43. RS Reis, AG Pereira, BC Neves, DM Freire, Gene regulation of rhamnolipid production in pseudomonas aeruginosa–a review. *Bioresour. Technol.* **102**, 6377–6384 (2011).
44. M Deforet, D Van Ditmarsch, C Carmona-Fontaine, JB Xavier. Hyperswarming adaptations in a bacterium improve collective motility without enhancing single cell motility. *Soft matter* **10**(14), 2405-13 (2014)
45. T Kohler, L Curty, F Barja, C Van Delden, and J Pechère. Swarming of *Pseudomonas aeruginosa* is dependent on cell-to-cell signaling and requires flagella and pili. *J. Bacteriol.* **182**(21), 5990-5996 (2000).
46. J Yan, H Monaco, JB Xavier, The ultimate guide to bacterial swarming: an experimental model to study the evolution of cooperative behavior. *Annu. Rev. Microbiol. 73*, 293–312 (2019).
47. AN Ebrahimi, D Or, Microbial dispersal in unsaturated porous media: Characteristics of motile bacterial cell motions in unsaturated angular pore networks. *Water Resour. Res.* **50**(9), 7406-29 (2014).
48. YJ Chuah, et al., Simple surface engineering of polydimethylsiloxane with polydopamine for stabilized mesenchymal stem cell adhesion and multipotency. *Sci. Reports* **5**, 1–12 (2015).
49. L de Vargas Roditi, KE Boyle, JB Xavier. Multilevel selection analysis of a microbial social trait. *Mol. Syst. Biol.* **9**(1), 684 (2013).
50. BM Doube, PM Stephens, CW Davoren, MH Ryder. Interactions between earthworms, beneficial soil microorganisms and root pathogens. *Appl. Soil Ecol.* **1**(1), 3-10 (1994).
51. AS Brown *et al.*, Cooperation between monocyte-derived cells and lymphoid cells in the acute response to a bacterial lung pathogen. *PLoS Pathog.* **12**(6):e1005691 (2016).
52. Y Tan, JT Gannon, P Baveye, M Alexander. Transport of bacteria in an aquifer sand: Experiments and model simulations. *Water Resour. Res.* **30**(12), 3243-52 (1994).
53. JW Foppen, A Mporokoso, JF Schijven. Determining straining of Escherichia coli from breakthrough curves. *J. Contam. Hydrol.* **76**(3-4), 191-210 (2005).
54. BN Sulman, RP Phillips, AC Oishi, E Shevliakova, SW Pacala. Microbe-driven turnover offsets mineral-mediated storage of soil carbon under elevated CO 2. *Nat. Clim. Change* **4**(12), 1099-102 (2014).
55. WR Wieder, GB Bonan, SD Allison. Global soil carbon projections are improved by modelling microbial processes. *Nat. Clim. Change* **3**(10),909-12 (2013).
56. JQ Yang, X Zhang, IC Bourg, HA Stone. 4D imaging reveals mechanisms of clay-carbon protection and release. *Nat. Commun.* **12**(1), 1-8 (2021).
57. NG Karanth, PG Deo, NK Veenanadig. Microbial production of biosurfactants and their importance. *Curr. Sci.* **10**, 116-26 (1999).
58. TT Nguyen, NH Youssef, MJ McInerney, DA Sabatini. Rhamnolipid biosurfactant mixtures for environmental remediation. *Water Res.* **42**(6-7),1735-43 (2008).
59. L Rodrigues, H Van der Mei, J Teixeira, and R Oliveira. Biosurfactant from *Lactococcus lactis* 53 inhibits microbial adhesion on silicone rubber. *Appl. Microbiol. Biotechnol.* **66**(3), 306-311 (2004).
60. P Saravanakumari, K Mani. Structural characterization of a novel xylolipid biosurfactant from *Lactococcus lactis* and analysis of antibacterial activity against multi-drug resistant pathogens. *Bioresour. Technol.* **101**(22), 8851-4 (2010).
61. B Lesic, LG Rahme, Use of the lambda red recombinase system to rapidly generate mutants in *Pseudomonas aeruginosa*. *BMC Mol. Biol*. **9**, 20 (2008).
62. Y Rotenberg, L Boruvka, A Neumann, Determination of surface tension and contact angle from the shapes of axisymmetric fluid interfaces. *J. Colloid Interface Sci.* **93**, 169–183 (1983).